International Journal of Heat and Mass Transfer 108 (2017) 2417–2432

Contents lists available at ScienceDirect

International Journal of Heat and Mass Transfer

journal homepage: www.elsevier.com/locate/ijhmt

Flow boiling heat transfer of R134a and low GWP refrigerants in a horizontal micro-scale channel

Daniel Felipe Sempértegui-Tapia [a,*], Gherhardt Ribatski [b]

[a] College of Engineering, Design and Physical Science, Brunel University of London, Uxbridge, London, UK
[b] Heat Transfer Research Group, Escola de Engenharia de São Carlos (EESC), University of São Paulo (USP), São Carlos, SP, Brazil

ARTICLE INFO

Article history:
Received 11 October 2016
Received in revised form 23 December 2016
Accepted 12 January 2017

Keywords:
Two-phase flow
Heat transfer coefficient
Micro-scale channels
R1234ze(E)
R1234yf
R600a
Low GWP

ABSTRACT

The present paper presents an investigation of the effects of the refrigerant type on the heat transfer coefficient during flow boiling inside micro-scale channels. Experimental results for R134a, R1234ze(E), R1234yf and R600a for flow boiling in a circular channel with internal diameter of 1.1 mm are presented. The experimental database comprises 3409 data points covering mass velocities ranging from 200 to 800 kg/m^2 s, heat fluxes from 15 to 145 kW/m^2, saturation temperatures of 31 and 41 °C, and vapor qualities from 0.05 to 0.95. The experimental data were parametrically analysed and the effects of the experimental parameters (heat flux, mass velocity, saturation temperature and working fluid) identified. Subsequently, the experimental data were compared against the most quoted predictive methods from literature, including macro and micro-scale methods. Based on the broad database obtained in the present study, an updated version of the predictive method of Kanizawa et al. (2016) was proposed. The updated version provided accurate predictions of the present experimental database, predicting more than 97% and 86% of the results within error bands of ±30 and ±20%, respectively.

1. Introduction

In the last two decades, several studies were performed concerning flow boiling inside micro-scale channels. However, it should be mentioned that the majority of these studies was performed for HFCs refrigerants as observed in the review of Kim and Mudawar [2]. In 1997, the Kyoto Protocol has established the gradual replacement of HFCs by refrigerants with global warming potential (*GWP*) less than 150. In this context, a new demand was generated for fluids that could substitute the HFCs. According to Calm [3] and Mota-Babiloni et al. [4], the potential substitutes for HFCs are natural refrigerants (hydrocarbons, CO_2 and ammonia), hydrofluoroolefins (R1234yf, R1234ze(E), R1234ze(Z) and R1233zd(E)) and mixtures of HFCs and hydrofluoroolefins (HFOs).

Table 1 shows a comparison of the principal properties of the HFOs (R1234ze(E) and R1234yf), the hydrocarbon (R600a) and the refrigerant R134a. According to this table, the HFOs and the hydrocarbon meet the environmental requirements by having an almost negligible *GWP* and a null *ODP*. The hydrocarbon R600a presents a latent heat of vaporization higher than the HFOs and R134a, implying on the need of lower mass velocities to dissipate the same amount of heat. It can also be observed in this table that the properties of the HFOs and the R134a are relatively close, confirming the HFOs as potential substitutes of the R134a. Moreover, it should be highlighted the fact that the R600a presents a saturated vapor density between three and four times lower than the HFOs and the R134a, which implies a higher vapor phase velocity during the flow boiling and, consequently, a higher pressure drop compared to the other fluids, as reported by Sempértegui-Tapia and Ribatski [5].

In the last few years, experimental results concerning flow boiling of natural refrigerants and HFOs have been reported in literature. However, the majority of them correspond to data for conventional channels (D > 3 mm). Therefore, it is not surprising the fact that is still not clear if the predictive methods available in the literature are capable to predict the HTC of these fluids under micro-scale conditions. Table 2 describes studies from literature concerning the evaluation of two-phase heat transfer coefficient for low GWP refrigerants in micro-scale single channels. Copetti et al. [6], Choi et al. [7], Del Col et al. [8] and de Oliveira et al. [9] performed experiments for flow boiling of hydrocarbons in micro-scale channels. Copetti et al. [6] and Choi et al. [7] reported that the heat transfer coefficient decreases with increasing vapor qualities, from vapor quality values of 0.3–0.4. On the other hand, Del Col et al. [8] and de Oliveira et al. [9] reported that the HTC increases with increasing vapor quality until conditions close to

* Corresponding author.
E-mail addresses: dsempertegui@hotmail.com (D.F. Sempértegui-Tapia), ribatski@sc.usp.br (G. Ribatski).

http://dx.doi.org/10.1016/j.ijheatmasstransfer.2017.01.036
0017-9310/

Nomenclature

A	area, m^2
Bd	Bond number, dimensionless
D	diameter, m
F	enhancement factor, dimensionless
G	mass velocity, kg/m^2 s
i	enthalpy, J/kg
h	heat transfer coefficient, kW/m^2 K
i	specific enthalpy, kJ/kg
I	electrical current, A
L	length, m
$\dot{M}$	mass flow rate, kg/s
MAE	Mean Absolute Error, %
MW	molecular weight, kg/kmol
p	pressure, kPa
P	electrical power, W
Q	heat, W
Ra	arithmetical mean roughness, μm
Re	Reynolds number, dimensionless
S	suppression factor, dimensionless
T	temperature, °C
V	voltage, V
We	Weber number, dimensionless
x	vapor quality, dimensionless
X	Lockhart and Martinelli parameter
z	position along the tube, m

Greek letters

α	void fraction, dimensionless
η	parcel of data predicted within a certain error band, %
ϕ	heat flux, kW/m^2
μ	dynamic viscosity, Pa s
ρ	density, kg/m^3
σ	surface tension, N/m

Subscripts

1ϕ	single-phase
2ϕ	two-phase
eff	effective
env	environment
exp	experimental
in	inlet
int	internal
loss	loss
L	saturated liquid phase
G	saturated gas phase
LG	difference between vapor and liquid properties
nb	nucleate boiling
out	outlet
ph	pre-heater
pred	predicted
sat	saturation
ts	test section

Table 1
Characteristics of the refrigerants at a saturation temperature of 25 °C.

Properties	R134a	R1234ze(E)	R1234yf	R600a
MW [g/mol][a]	102	114	114	58.12
P_{sat} [kPa][a]	665.8	500.1	682.5	350.4
ρ_L [kg/m^3][a]	1207	1162	1092	549.9
ρ_G [kg/m^3][a]	32.37	26.76	37.94	9.123
μ_L [μPa s][a]	194.4	203.4	161.1	150
i_{LG} [kJ/kg][a]	177.8	166.5	146.4	329.1
σ [mN/m][a]	8.03	8.88	6.17	9.86
GWP	1300	7	4	3
ODP	0	0	0	0

[a] Values acquired from Engineering Equation Solver, EES V10.005.

the dryout and thereby, they pointed out convective effects as predominant mechanism for intermediary and high vapor qualities. Copetti et al. [6] found that the method of Kandlikar and Balasubramanian [10] provided the best predictions of their data. Instead, de Oliveira et al. [9] and Del Col et al. [8] pointed out the methods of Kim and Mudawar [11] and Thome et al. [12] as the most accurate ones, respectively. Among six predictive methods from literature, Choi et al. [7] reported the method of Gungor and Winterton [13] as the one that provided the best predictions of their data.

Saitoh et al. [14], Li et al. [16], Mortada et al. [17], Tibiriça et al. [18], Del Col et al. [19], Choi et al. [7] and Anwar et al. [20] gathered experimental results for the heat transfer coefficient of hydrofluo-

Table 2
Experimental flow boiling studies for low GWP fluid in horizontal micro-scale channels.

Author(s)	Fluid	D [mm]	G [kg/m^2 s] ϕ [kW/m^2]	Best reported prediction method
Saitoh et al. [14]	R1234yf	2	100–400 6–24	Saitoh et al. [15]
Li et al. [16]	R1234yf	2	100–400 6–24	No one
Mortada et al. [17]	R1234yf	1.1	20–100 2–15	No one - New method
Tibiriça et al. [18]	R1234ze(E)	1, 2.2	50–1500 10–300	Saitoh et al. [15]
Del Col et al. [19]	R1234yf	0.96	200–600 15–65	No one
Copetti et al. [6]	R600a	2.6	240–440 44–95	Kandlikar and Balasubramanian [10]
Choi et al. [7]	R744, R717, R290, R1234yf	1.5, 3	50–600 5–60	Gungor and Winterton [13]
Del Col et al. [8]	R290	0.96	100–600 5–315	Thome et al. [12]
Anwar et al. [20]	R1234yf	1.6	100–500 5–130	Gungor and Winterton [13] Mahmoud and Karayiannis [21]
De Oliveira et al. [9]	R600a	1	240–480 5–60	Kim and Mudawar [11]

roolefins (R1234ze(E) and R1234yf). Mortada et al. [17] reported HTCs for R1234yf about 40% higher than the one for R134a. Tibiriça et al. [18], Del Col et al. [19] and Anwar et al. [20] verified almost similar heat transfer coefficients for the HFO and R134a. Saitoh et al. [14], Li et al. [16] and Choi et al. [7] reported the predominance of the nucleate boiling effects for R1234yf. Anwar et al. [20] reported that their database for the heat transfer coefficient is satisfactorily predicted by the methods of Gungor and Winterton [13] and Mahmoud and Karayiannis [21]. Instead, Tibiriça et al. [18] reported the method of Saitoh et al. [15] as the most accurate to predict their experimental database. No one of the methods from literature evaluated by Mortada et al. [17] provided reasonable prediction of their experimental data, so, they developed a new correlation.

In addition to the fluids listed in Table 2, it is important to highlight the work of Huang et al. [22] that, as far as the present authors know, is the only study for flow boiling of refrigerant R1233zd(E) inside microchannels. However, it is important to highlight that the present study is focused only on results for single channels, and the work of Huang et al. [22] was performed for a multichannel configuration, when additional thermal hydraulic effects are present such as thermal instabilities, back flows, and mal distribution.

According to this brief literature review, it can be concluded that there are reasonable discrepancies among data from independent laboratories and there is no consensus about the best method to be applied to predict the heat transfer coefficient during flow boiling of low GWP fluids in micro-scale channels. These facts indicate the need to perform careful experiments in order to obtain accurate data for low GWP fluids covering a wide range of experimental conditions, making possible the comparison of HTC values for different fluids. These data can be used in order to support the development of accurate predictive methods. In this context, the present paper concerns an experimental investigation on the effect of the fluid refrigerant on the flow boiling heat transfer coefficient. Experimental results for R134a, R1234ze(E), R1234yf and R600a in a circular channel with and internal diameter of 1.1 mm are presented. The experimental database comprises 3409 data points covering mass velocities ranging from 200 to 800 kg/m^2 s, heat fluxes from 15 to 145 kW/m^2, saturation temperatures of 31 and 41 °C, and vapor qualities from 0.05 to 0.95. The experimental data were parametrically analysed and the effects of the experimental parameters identified. Then, the experimental results were compared against the most quoted predictive methods from literature, including methods developed for macro-scale channels and methods specially developed for micro-scale channels. Additionally, an updated version of the predictive method of Kanizawa et al. [1] was proposed based on the broad database obtained in the present study. The updated method was not only able to predict accurately the experimental results, but also to capture the main behaviors of the data obtained in the present study.

2. Experimental apparatus

2.1. General description

The experimental setup is comprised of refrigerant and water circuits. The water circuit is intended to condense and subcool the working fluid. The refrigerant circuit is schematically shown in Fig. 1. In the refrigerant circuit, the test fluid is driven through the circuit by a self-lubricating oil-free micropump. The liquid flow rate is set by a frequency inverter acting on the micropump. Downstream the micropump, the mass flow rate is measured with a Coriolis flow meter. Upstream the pre-heater, the fluid inlet conditions are determined by a thermocouple and an absolute pressure transducer. Downstream the test section, a visualization section, a tube-in-tube heat exchanger, and a refrigerant tank are sequentially located. The heat exchanger is responsible for condensing the vapor created in the heated sections. Additional details of the experimental set up can be found in Tibiriçá and Ribatski [23] and Sempértegui-Tapia et al. [24].

2.2. Pre-heater and test section

A 490 mm horizontal AISI-304 stainless-steel tube, acquired from Goofellow Cambridge Limited, with external and internal diameters of 1.47 mm and 1.1 mm, respectively, forms the pre-heater and the test section. The arithmetical mean roughness of the tube was measured with the optical profiling system Wiko® NT1100 equipment, and a mean average surface roughness (Ra) of 0.289 μm was found based on three measurements along the test section length. Fig. 2 shows an image of the inner surface of the test section and the roughness profile obtained through the measurements.

The pre-heater and the test sections are 200 and 150 mm long, respectively. The pre-heater and the test section are heated by applying direct DC current to their surface and both sections are thermally insulated. The heating power is supplied to the test sections by independent DC power sources, controlled from the data acquisitions system. The preheater and the test and visualization sections are connected through junctions made of polyvinylidene fluoride (PVDF) specially designed and machined to match up their ends and keep a smooth and continuous internal surface. Once the fluid has left the test section, its temperature is determined from a 0.25 mm thermocouple whose hot junction is flush-mounted into the pipe wall. The corresponding absolute pressure is estimated from the inlet absolute pressure, p_{in}, and the total pressure drop given by a differential pressure transducer over the length comprising the preheater inlet and the test section outlet, Δp. The wall temperatures are measured through 0.25 mm K-type thermocouples fixed along the test section. There were installed ten thermocouples at five measuring cross-sections, one at the bottom and another on the top of the tube. Besides the thermocouples along the heated test section, there were positioned thermocouples 15 mm before and after the electrodes, these temperature measurements are used to estimate the local saturation temperature along the test section. All the thermocouples at the test section were fixed tightly against the tube surface. A detailed scheme of the pre-heater and the test section is shown in Fig. 3.

2.3. Experimental conditions

Table 3 presents a summary of the experimental conditions evaluated in the present study.

3. Data reduction, experimental validation and uncertainties

3.1. Data reduction

3.1.1. Mass velocity

Mass velocity was calculated as the ratio between the mass flow rate measured by the Coriolis mass flow meter and the internal cross sectional area of the tube, according to the following equation:

$$G = \frac{\dot{M}}{A_{\text{int}}} \tag{1}$$

The cross-sectional area of the circular tube is calculated as follows:

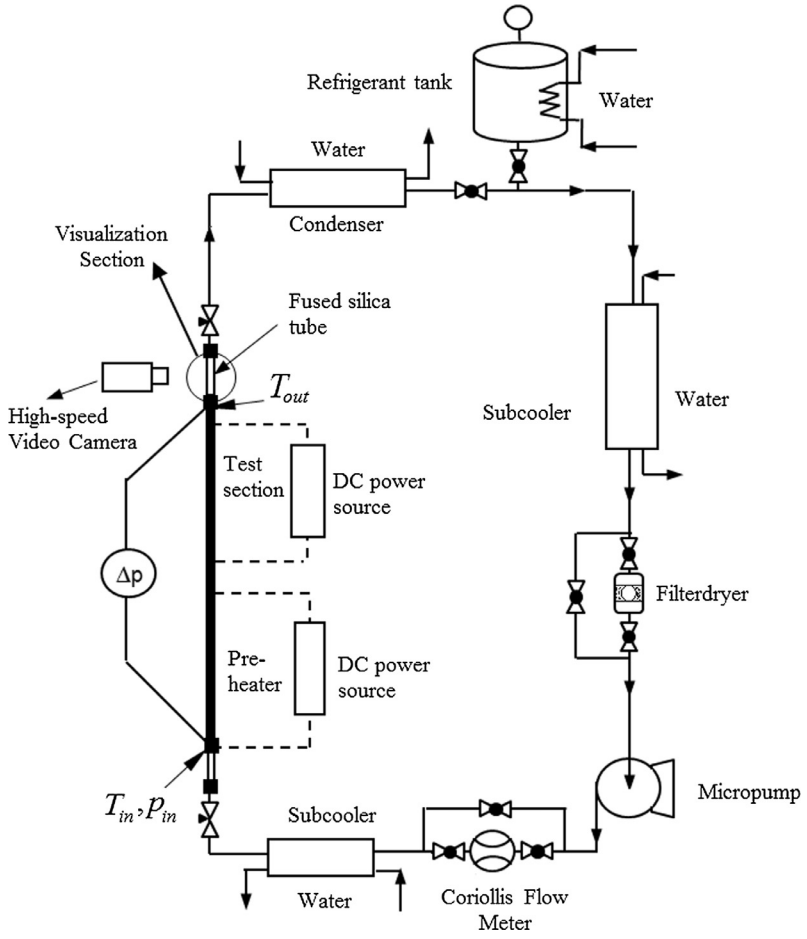

Fig. 1. Schematic diagram of the refrigerant circuit.

$$A_{\text{int}} = \frac{\pi D_{\text{int}}^2}{4} \tag{2}$$

3.1.2. Heat flux

The heat flux at the test section, ϕ_{ts}, is evaluated as the ratio of the effective electrical power and the internal superficial area of the heated tube length as follows:

$$\phi_{ts} = \frac{P_{ts,eff}}{\pi D_{\text{int}} L_{ts}} \tag{3}$$

The effective electrical power is given as the difference between the electrical power (product between the voltage and the electric current provided by the DC power source) applied to the test section and the heat losses to the environment:

$$P_{\text{ts},eff} = V_{ts} I_{ts} - Q_{\text{ts},loss} \tag{4}$$

The heat losses to the environment are estimated through experiments characterized by the imposition of a heating power on the test section without refrigerant, and by evaluation of the temperature difference between its heated surface and the environment after the heating process reach steady state. Once steady state condition is achieved, it was assumed that all the heating electrical power is dissipated to the environment as heat losses. Taking into account this hypothesis, experimental values for the temperature difference with varying the heating electrical power were acquired and a curve fitting performed, given as follows:

$$Q_{\text{ts},loss} = 0.0112 \cdot (\overline{T}_w - T_{env}) - 0.0625 \tag{5}$$

3.1.3. Vapor quality

The local vapor quality along the test section was determined through energy balances over the pre-heater and the test section according to the following equations:

$$x(z) = \frac{1}{i_{LG}(z)} \left[\frac{P_{ph} + P_{ts}(z)}{\dot{M}} + (i_{L,in} - i_{L,in}(z)) \right] \tag{6}$$

$$P_{ts}(z) = \phi_{ts} \pi D_{\text{int}} z \tag{7}$$

where $i_{L,in}$ is the enthalpy of the liquid at the inlet of the pre-heater, $i_{L,in}(z)$ and $i_{LG,in}(z)$ are the enthalpy of the saturated liquid and the latent heat of vaporization corresponding to the local saturation temperature at the position z, respectively.

3.1.4. Local saturation temperature

The local saturation temperature of the refrigerant was estimated from the local saturation pressure calculated as follows:

$$p_{sat}(z) = p_{in} - \Delta p_{in-z} \tag{8}$$

where p_{in} is the inlet saturation pressure estimated from the inlet temperature, given by the thermocouple located just upstream the first electrode in the test section. $\Delta p_{in\text{-}z}$ is the pressure drop along the test section length from the thermocouple used to evaluate p_{in} to the position z at which the heat transfer coefficient is being evaluated (see Fig. 3). The value of $\Delta p_{in\text{-}z}$ is estimated through an iterative process as the sum of accelerational and frictional components of the pressure drop over 100 discrete elements comprising the corresponding test section length. In this procedure, the trans-

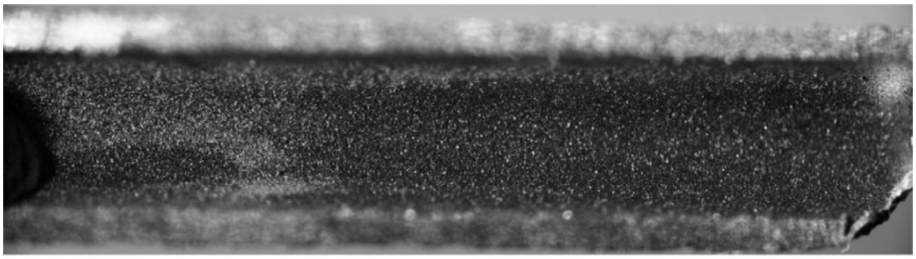

(a)

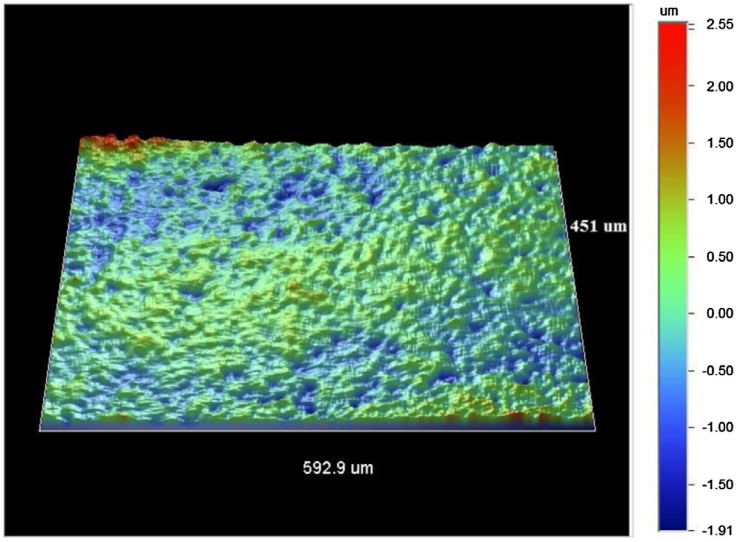

(b)

Fig. 2. (a) Image of the inner tube surface, (b) 3D image of the microchannel inner surface taken by the optical profiling system Wiko® NT110.

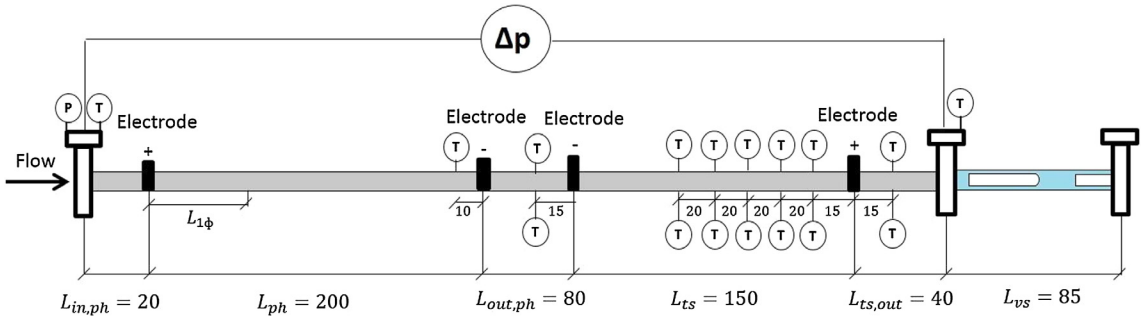

Fig. 3. Schematic of the pre-heater section and the test section.

Table 3
Experimental conditions of the present study.

Working fluid	R134a	R1234ze(E)	*R1234yf*	R600a
D [mm]	1.1	1.1	1.1	1.1
ϕ [kW/m^2]	15–85	15–95	15–55	15–145
G [kg/m^2 s]	200–800	100–500	100–400	200–500
T_{sat} [°C]	31, 41	31, 41	31, 41	31, 41
x [–]	0–0.91	0–0.91	0–0.91	0–0.93
h [kW/m^2 °C]	4.73–21.3	3.26–17.31	4.24–14.42	2.55–32.41

port and thermodynamic properties were calculated locally based on the average saturation pressure of each element.

The acceleration pressure drop was estimated according to:

$$\Delta p_{acc} = G^2 \left\{ \left[\frac{x^2}{\rho_G \alpha} + \frac{(1-x)^2}{\rho_L (1-\alpha)} \right]_z - \left[\frac{x^2}{\rho_G \alpha} + \frac{(1-x)^2}{\rho_L (1-\alpha)} \right]_{in} \right\} \quad (9)$$

where the subscripts *in* and *z* refer to the position at the inlet of the test section and at the position z, respectively. The superficial void fraction was estimated through the method recently proposed by Kanizawa and Ribatski [25], which is based on the principle of minimization of energy dissipation, analogous to the procedure initially proposed by Zivi [26]. This method was chosen because it provided

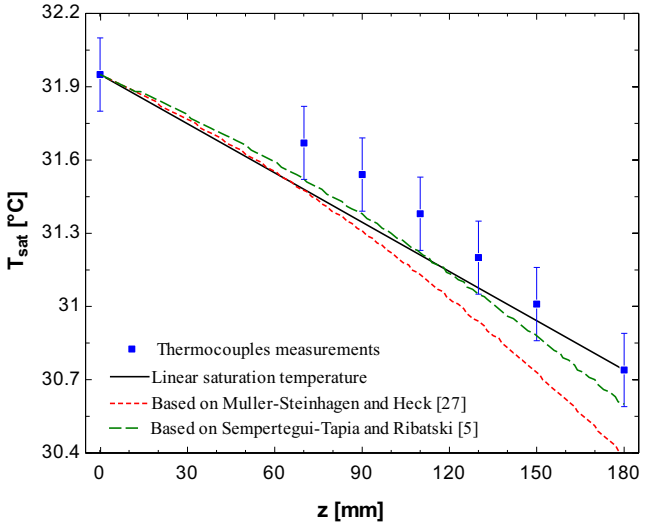

Fig. 4. Comparison among experimental results and different methods to estimate the local saturation temperature.

the best estimative of a broad experimental database (more than 3000 data) when compared with previous methods available in the literature.

The frictional pressure drop was estimated using the predictive method recently proposed by Sempértegui-Tapia and Ribatski [5]. This method was chosen based on the comparison of experimental and estimated local saturation temperatures under adiabatic conditions, illustrated in Fig. 4. According to this figure, the assumptions of a linear profile saturation temperature and values given by the method of Sempértegui-Tapia and Ribatski [5] provide results within the range of uncertainty of the temperature measurements. On the other hand, it can be observed higher discrepancies between the experimental values of the saturation temperature and the values estimated based on the predictive pressure drop method by Müller-Steinhagen and Heck [27]. It's worth to mention that the method by Sempértegui-Tapia and Ribatski [5] is based on the method by Müller-Steinhagen and Heck [27] and was developed considering a broad experimental database comprising the same fluids of the present study (R134a, R1234ze(E), R1234yf and R600a).

3.1.5. Heat transfer coefficient

The local heat transfer coefficient was calculated according to the Newton's cooling law as follows:

$$h(z) = \frac{\phi_{ts}}{T_{w,in}(z) - T_{sat}(z)} \tag{10}$$

where $T_{w,in}(z)$ is the inner wall temperature at the position z. This temperature is estimated according to Fourier's law based on the outer wall temperature measurements, considering one-dimensional conduction and uniform heat generation through Joule effect. In Eq. (10), $T_{sat}(z)$ is the local saturation temperature estimated as explained in Section 3.1.4.

3.2. Experimental validation

3.2.1. Single-phase pressure drop

Experimental tests for single-phase flows were previously performed in order to assure the accuracy of the measurements and evaluate the effective rate of heat losses and consequently the accuracy of the vapor quality estimative. Fig. 5 illustrates the single-phase pressure drop results for the four fluids. The flow is considered to be hydrodynamically developed at the inlet of the pre-heater. This hypothesis is based on the fact that the visualization section, located upstream the pre-heater (as shown in Fig. 1), is 100 mm long (approximately 100 times the tube internal diameter). As shown in Fig. 5, the laminar experimental data for pressure drop agree reasonably well with the theory of laminar flow (Hagen-Pouseuille). For turbulent flow, the method of Blasius [28] provided accurate predictions, resulting a mean absolute error (MAE) of 8.1%.

3.2.2. Single-phase heat transfer coefficient

Results for the heat transfer coefficient for single-phase flows are also analysed in order to validate energy balances along the pre-heater and the test section. The experimental heat transfer coefficient for single-phase flow was estimated using the last thermocouple placed on the test section in order to get a thermally fully developed condition for turbulent flow. Unfortunately, the test section length was not enough to achieve a thermally fully developed condition for laminar flow. Fig. 6 illustrates the experimental single-phase HTC and the corresponding predictions according to methods from literature. As noted in this figure, the correlation for thermally developing laminar flow of Siegel et al.

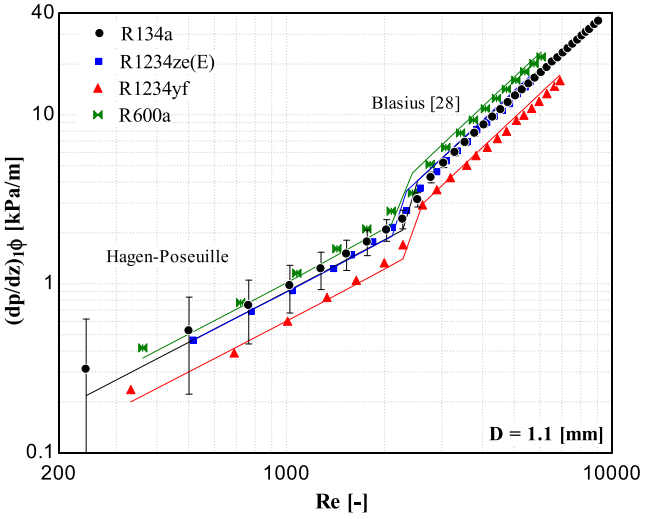

Fig. 5. Comparison between experimental and estimated results for single-phase pressure for circular channels.

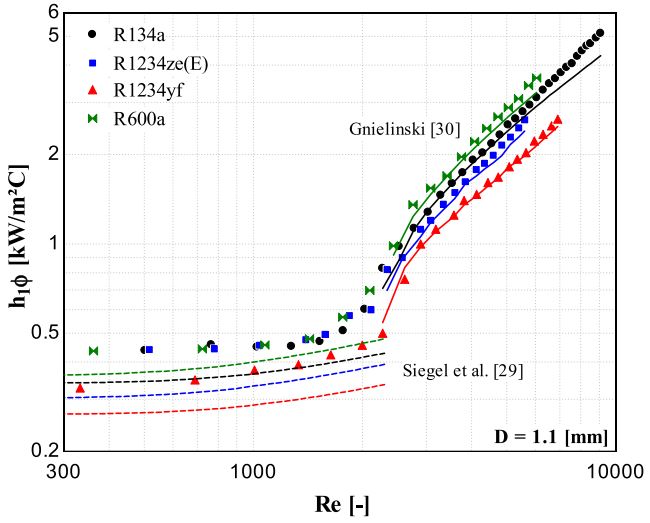

Fig. 6. Single-phase heat transfer coefficient.

Table 4
Uncertainty of measured and calculated parameters.

Measured parameter	Uncertainty	Calculated parameter	Uncertainty
D	20 μm	x	<5%
L_{ph}, L_{ts}	1 mm	G	<2%
p_{in}	4.5 kPa	$h_{2\phi}$ *for low* ϕ	7–18%
Δp	150 Pa	$h_{2\phi}$ *for high* ϕ	4–6%
P_{ph}, P_{ph}	0.8%		
T	0.15 °C		
$\dot{M}$	0.1%		

[29] captures adequately the tendency of the experimental data. However, this correlation under-predict the experimental values in around 20%. For turbulent flow, the correlation of Gnielinski [30] agrees quite well with the experimental values for the four fluids. It can also be observed that the experimental transition from laminar to turbulent flow seems to occur for a Reynolds number between 2000 and 2500, which agrees with theory.

3.3. Uncertainties propagation

Temperature measurements were calibrated and the temperature uncertainty was evaluated according to the procedure suggested by Abernethy et al. [31]. Accounting for all instrument errors, uncertainties for the calculated parameter were estimated using the method of sequential perturbation according to Taylor and Kuyatt [32]. All the experimental uncertainties associated with the sensors and calculated parameters are listed in Table 4.

It is important to highlight that the experimental data were acquired only under stable conditions, characterized by temperature and pressure oscillations within the range of uncertainty of their measurements.

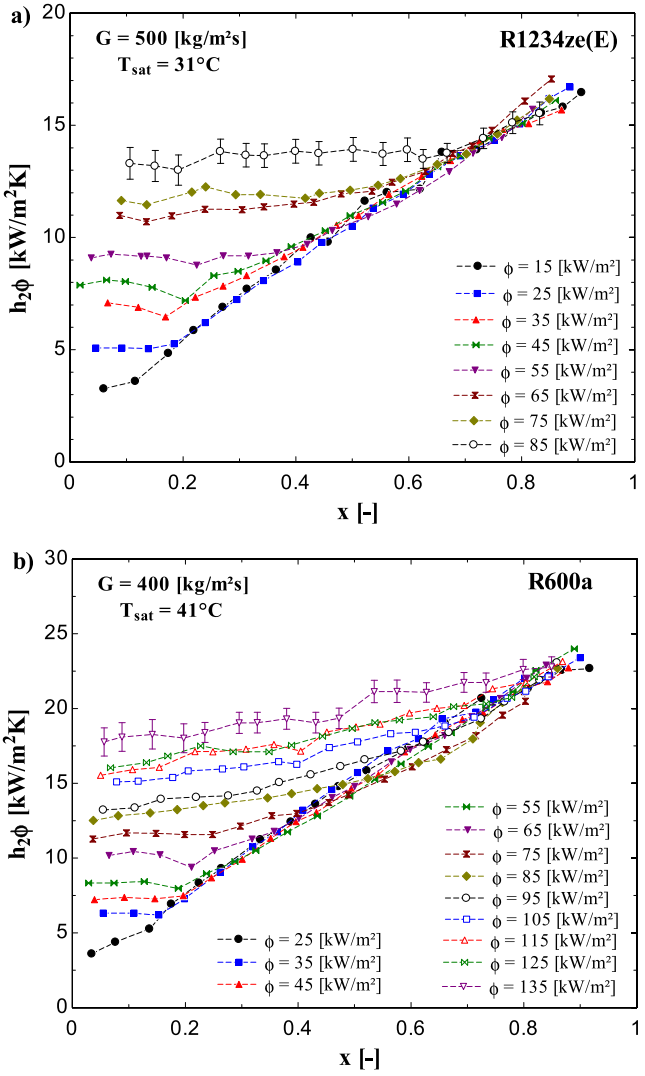

Fig. 7. Effect of the heat flux and vapor quality on the heat transfer coefficient, (a) R1234ze(E), (b) R600a.

4. Experimental results

4.1. Local two-phase heat transfer coefficient

In this item, the main trends observed in the present study for the heat transfer coefficient with the variation of the experimental parameters are presented and discussed.

4.1.1. Effect of the heat flux and quality vapor

Fig. 7 illustrates the effect of the heat flux and vapor quality on the heat transfer coefficient for the fluids R1234ze(E) and R600a. According to this figure, in general, the heat transfer coefficient increases with increasing heat flux for experimental conditions corresponding to low and intermediary vapor qualities. For high vapor qualities, the heat transfer coefficient becomes almost independent of the heat flux. Such behaviors seem to be associated to the predominance of nucleate boiling effects under conditions of high heat fluxes and low vapor qualities. The two-phase flow velocity increases with increasing vapor quality, implying on the suppression of nucleate boiling and enhancement of convective effects. The above mentioned mechanisms to explain flow boiling behaviors in micro-scale channels are a controversial point in the literature that however is corroborated by the results of Tibiriçá and Ribatski [33]. These authors observed bubble nucleation under conditions of elongated bubbles and annular flow patterns for flow boiling inside micro-scale channels. Kalani and Kandlikar [34] and Basu et al. [35] also observed the presence of bubble nucleation in small diameter channels. Recently, Chávez et al. [36] based on their study for flow boiling inside multi-channels observed for data obtained under conditions of progressive decrease of heat flux that the heat transfer coefficient decreases with reducing the heat flux despite of the apparent absence of bubble nucleation. This heat transfer coefficient behavior is typical of flow boiling heat transfer and does not of forced convection. Based on this fact, Chávez et al. [36] explained such behavior through the presence of microbubbles not perceptible through their high-speed camera and magnifying lens. It is important to highlight that mechanistic models for elongated bubbles and annular flow patterns and correlations based only on convective effects are not able to explain such behavior.

4.1.2. Effect of mass velocity

Fig. 8 illustrates the effect of mass velocity on the heat transfer coefficient under different experimental conditions for fluids R1234yf and R600a. According to this figure, the HTC increases with increasing mass velocity for intermediary and high vapor qualities, conditions that convective effects prevails. For low vapor qualities, the nucleate boiling effect is dominant; hence, it can be observed heat transfer coefficient behavior almost independent of the mass velocity.

4.1.3. Effect of saturation temperature

Fig. 9 illustrates the effect of saturation temperature on the heat transfer coefficient. According to the figure, for the fluid R134a, the HTC increases from 5 to 15% with increasing the saturation temperature from 31 to 41 °C. On the other hand, for R600a, the heat

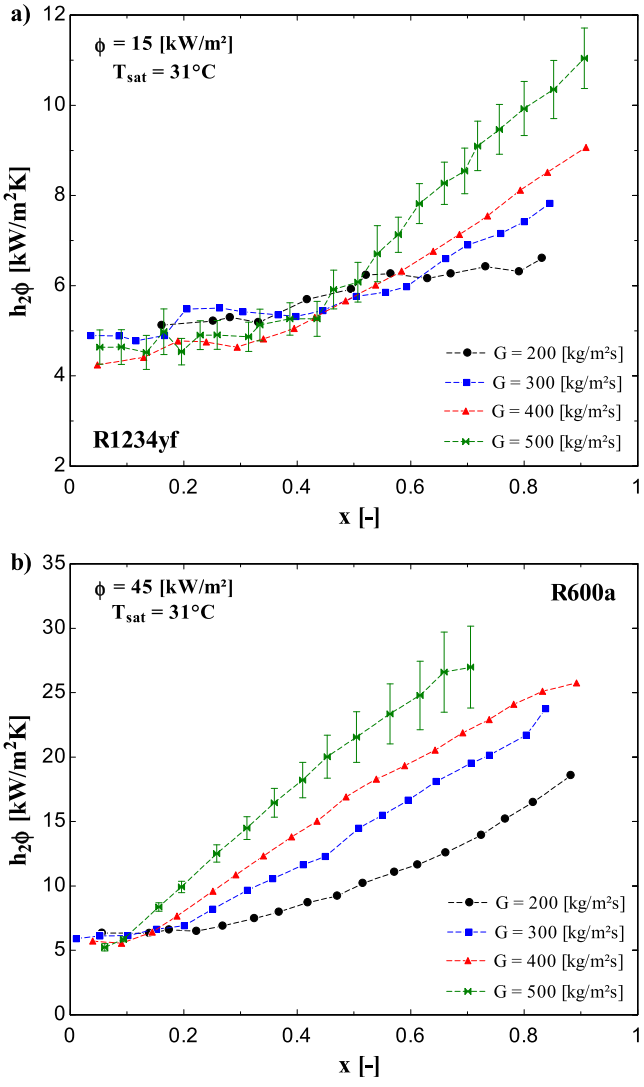

Fig. 8. Effect of the mass velocity on the heat transfer coefficient, (a) R1234yf, (b) R600a.

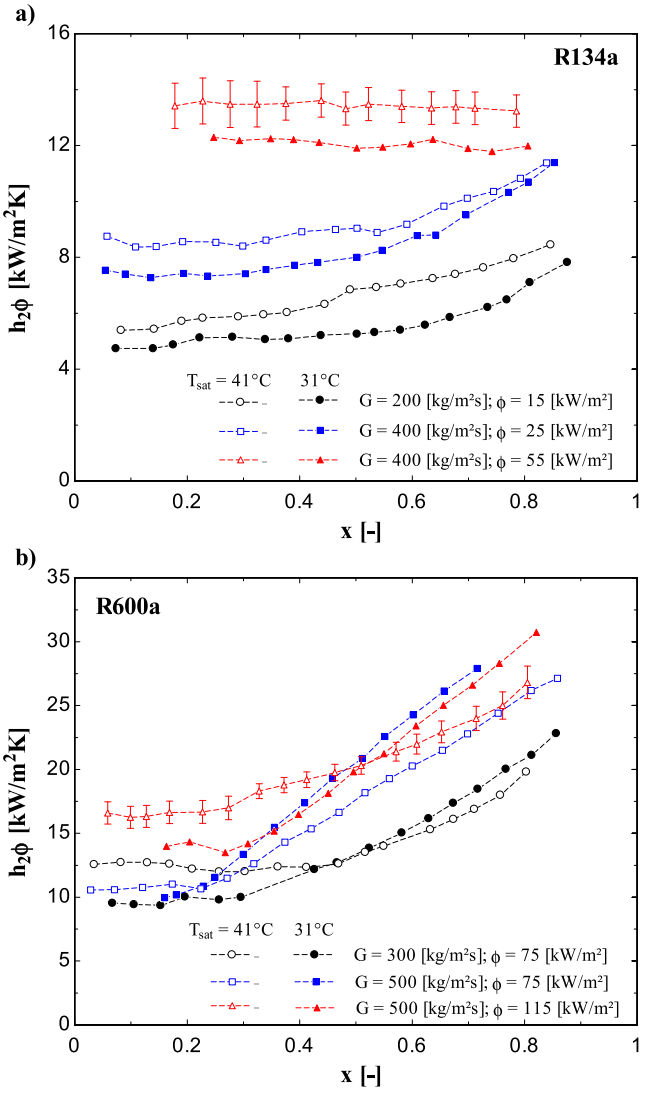

Fig. 9. Effect of the local saturation temperature on the heat transfer coefficient, (a) R134a, (b) R600a.

transfer coefficient increases with increasing saturation temperature at low vapor qualities. An opposite behavior is observed for high vapor qualities. The vapor quality at which the trend is shifted seems to be affected by the heat flux and mass velocity. By increasing the heat flux and decreasing the mass velocity, the vapor quality corresponding to the shift of trend is postponed to higher values. An opposite behavior occurs by decreasing heat flux and increasing mass velocity.

4.1.4. Effect of working fluid

Figs. 10 and 11 illustrate comparisons of the heat transfer coefficients for R134a, R1234yf, R1234ze(E) and R600a for saturation temperatures of 31 and 41 °C, respectively.

According to Fig. 10, the heat transfer coefficient of R134a and R1234yf presents close results and almost similar trends. Moreover, the heat transfer coefficient of R134a is about 2–10% higher than R1234yf for low heat fluxes (15 kW/m^2), while for high heat fluxes (45 kW/m^2) the HTC of R1234yf is about 6–10% higher than the heat transfer coefficient of the R134a. This result agrees with Del Col et al. [19] and Anwar et al. [20], who also reported almost similar values of the heat transfer coefficient for R1234yf and R134a. For low vapor qualities, the HTC of R1234ze(E) is lower than the heat transfer coefficient of R134a and R1234yf. This difference increases with increasing heat flux. For high vapor qualities, the HTC of R1234ze(E) is higher than the heat transfer coefficient of R134a.

On the other hand, the heat transfer coefficient of R600a, although lower than R134a and HFOs for vapor qualities lower than 0.2, increases significantly with increasing the vapor quality, reaching values up to 120% higher than the other fluids for $x > 0.8$. Such a behavior seems to be related to the predominance of convective effects for R600a because the specific vapor volume of this refrigerant is about four times higher than the other fluids, as indicated in Table 1. This fact implies on the enhancement of flow acceleration and of convective effects along the test section as result of the evaporation process. As the two-phase flow velocity increases the temperature gradient of the fluid near the tube wall also increases, suppressing nucleate boiling effects.

Furthermore, for low heat fluxes and vapor qualities higher than 0.3, the heat transfer main mechanism seems to be related to convective effects for all fluids (see Fig. 10). By increasing the heat flux and keeping the mass velocity and saturation temperature constant, the heat transfer dominant mechanism for R134a, R1234ze (E) and R1234yf becomes nucleate boiling. However, for R600a and under the same experimental conditions the dominant mech-

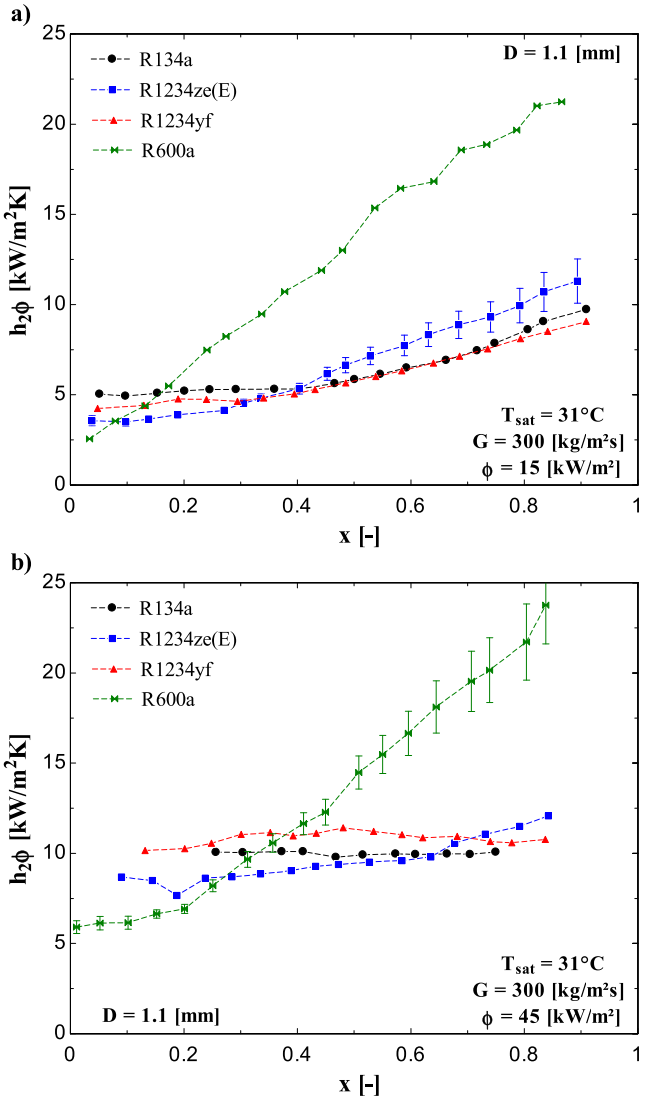

Fig. 10. Effect of the working fluid on the local heat transfer coefficient for T_{sat} = 31 °C.

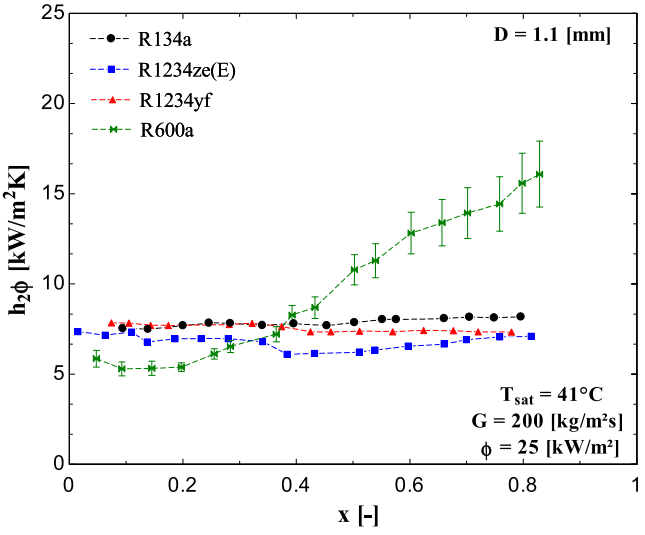

Fig. 11. Effect of the working fluid on the local heat transfer coefficient for T_{sat} = 41 °C.

anism is still associated to convective effects. It is worth to mention that this behavior for the isobutane differ significantly from the results by Copetti et al. [6], but agrees with the results of de Oliveira et al. [9].

According to Fig. 11, experimental results for the fluids R134a, R1234ze(E) and R1234yf indicate a predominance of the nucleate boiling effects for a saturation temperature of 41 °C. While for the isobutane the prevailing heat transfer mechanism seems to be still related to convective effects for vapor qualities higher than 0.2. It also can be observed that the heat transfer coefficient for the R1234ze(E) is lower than the HTC for the fluid R134a and R1234yf, regardless the vapor quality range.

4.2. Assessment of predictive methods

The capability of the methods from literature to predict the data obtained in the present study was evaluated by comparing their predictions with the corresponding experimental results. The comparison was performed based on the resulting statistical parameters and on the evaluation of the main heat transfer trends.

4.2.1. Statistical evaluation of the predictive methods

Table 5 presents de mean absolute error (MAE) and the parcels of data predicted within an error band of ±30% (η) obtained from the comparisons between predictive methods and the experimental database. These statistical parameters were calculated considering the data for each fluid and the overall database.

For the comparisons involving the overall database, the methods of Kanizawa et al. [1] and Kim and Mudawar [11] provided the best predictions of the experimental database, predicting 82.0 and 81.1% of the data within an error band of ±30%, respectively. The methods of Kew and Cornwell [41] and Sun and Mishima [44] also provided reasonable agreement with the experimental data, predicting 78.9% and 76.8% of the overall database within an error band of 30%, respectively. Chen [37], Lazareck and Black [38], Liu and Winterton [39], Zhang et al. [42], Saitoh et al. [15] and Mahmoud and Karayiannis [21] performed relatively well, providing mean absolute errors between 22.4 and 27%. The methods by Tran et al. [40], Thome et al. [12], Bertsch et al. [43] and Li and Wu [45] provided MAEs higher than 31% and a η lower than 55%. Although not listed in Table 5, it is worth to mention that the methods of Warrier et al. [46], Kandlikar and Balasubramanian [10], Oh and Son [47], Oh et al. [48], Cioncolini and Thome [49] and Costa-Patry and Thome [50] were also compared with the database obtained in the present study. In general, these methods predicted less than 20% of the database within an error band of ±30%.

The macro-scale predictive method of Chen [37] provided accurate predictions of the data of R134a and performed relatively well for R1234ze(E) and R1234yf. Liu and Winterton [39] ended up being the most adequate predictive method for the hydrocarbon R600a, predicting 69.4% of the data within an error band of ±30%. However, it is important to mention that despite providing the best predictions, a $\eta_{30\%}$ around 65–70% is not satisfactory.

The method of Thome et al. [12] performed relatively well for the fluid R134a and R1234ze(E), but failed to predict the experimental data for R1234yf and R600a. Tran et al. [40] and Zhang et al. [42] provided reasonable predictions of the results of R1234yf and R134a, respectively. Li and Wu [45] performed relatively well for R1234yf and R134a. Mahmoud and Karayiannis [21] provided reasonable predictions for R1234yf and performed relatively well for R134a and R1234ze(E). The method of Bertsch et al. [43] wasn't able of providing reasonable predictions of any of the fluids evaluated in the present study.

Despite being developed based on data for vertical flow of R113, the method of Lazareck and Black [38] agreed reasonably well with the experimental data for R134a and R1234yf. The method of Kew

Table 5
Statistical parameters resulting from the comparison of the experimental data with the predictive methods.[a]

Predictive method	Fluid #Data	R134a 772	R1234ze(E) 847	R1234yf 475	R600a 1315	Overall 3409
Chen [37]	MAE	**16.9%**	20.8%	22.5%	26.6%	22.4%
	η	**90.5%**	77.4%	74.1%	57.7%	72.3%
Lazareck and Black [38]	MAE	22.1%	20.4%	**17.6%**	28.3%	23.4%
	η	75.6%	76.6%	**88.0%**	59.8%	71.4%
Liu and Winterton [39]	MAE	27.7%	28.8%	32.7%	22.2%	26.5%
	η	58.4%	53.0%	25.1%	69.4%	56.6%
Tran et al. [40]	MAE	43.2%	31.4%	**11.8%**	55.7%	40.7%
	η	6.7%	59.6%	**94.5%**	4.3%	31.2%
Kew and Cornwell [41]	MAE	**16.4%**	**15.9%**	**10.2%**	24.2%	**18.4%**
	η	**82.9%**	**83.7%**	**96.6%**	67.1%	78.9%
Thome et al. [12]	MAE	20.5%	25.6%	30.3%	41.2%	31.1%
	η	76.7%	65.2%	49.9%	36.1%	54.5%
Zhang et al. [42]	MAE	21.1%	26.5%	25.7%	31.4%	27.0%
	η	**81.7%**	61.9%	63.2%	50.5%	62.1%
Saitoh et al. [15]	MAE	22.1%	**18.4%**	**15.8%**	31.5%	23.9%
	η	**80.6%**	79.5%	**88.6%**	54.5%	71.3%
Bertsch et al. [43]	MAE	39.2%	38.5%	35.7%	39.5%	38.6%
	η	15.2%	26.6%	28.8%	39.0%	29.1%
Sun and Mishima [44]	MAE	**11.6%**	**15.5%**	**8.0%**	27.3%	**18.1%**
	η	**86.8%**	**83.9%**	**97.3%**	59.1%	76.8%
Li and Wu [45]	MAE	23.9%	26.8%	20.6%	48.9%	33.8%
	η	70.6%	60.0%	77.3%	18.9%	48.9%
Kim and Mudawar [11]	MAE	**11.0%**	**13.2%**	**10.0%**	23.8%	**16.8%**
	η	**94.8%**	**88.0%**	**96.8%**	62.9%	**81.1%**
Mahmoud and Karayiannis [21]	MAE	23.9%	25.9%	22.3%	29.2%	26.2%
	η	69.4%	65.9%	**81.9%**	57.0%	66.3%
Kanizawa et al. [1]	MAE	**18.4%**	**13.2%**	**16.7%**	22.8%	**18.4%**
	η	**90.0%**	**90.8%**	**98.7%**	65.7%	**82.0%**

[a] Bold numbers indicate a MAE below 20% and more than 80% of the data predicted within the ±30%.

and Cornwell [41] whose development was based on the work of Lazareck and Black [38] provided good predictions of the data for R134a, R1234ze(E) and R1234yf. However, considering that this method is based on the predominance of nucleate boiling effects, it is not surprising that the method of Lazareck and Black [38] does not predicts satisfactorily the results of R600a, fluid for which convective effects are predominant, as discussed in Section 4.1.4. The methods of Sun and Mishima [44] and Kim and Mudawar [11] provided accurate predictions of the experimental databases of the fluids R134a, R1234ze(E) and R1234yf. However, both methods failed to predict the experimental data of R600a, probably due the fact that none of these methods includes R600a in the experimental database used for their development. The predictions provided by the method of Saitoh et al. [15] are in good agreement with the experimental data for R134a, R1234ze(E) and R1234yf. It is important to highlight that the method of Saitoh et al. [15] was developed based on a database containing experimental results only for R134a and tube diameters from 0.51 to 10.92 mm. For the same fluids, the method of Kanizawa et al. [1] predicted more than 90% of the experimental data within an error band of ±30% while Saitoh et al. [15], in general, provided a value of η higher than 79%. The method of Kanizawa et al. [1] was developed based on the work of Saitoh et al. [15].

Fig. 12 illustrates comparisons between the experimental database segregated according to the fluids with the predictive methods of Kew and Cornwell [41], Sun and Mishima [44], Kim and Mudawar [11] and Kanizawa et al. [1]. According to this figure, the four methods mostly underestimate a significant parcel of the experimental data independently of the fluid and heat transfer coefficient range.

4.2.2. Trend evaluation of the predictive methods

Since a good predictive method should be not only statistically accurate, but also be able of capturing the main trends of the experimental results, Fig. 13 displays the evolution of the heat transfer coefficient with the vapor quality according to the predictive methods and the experimental data.

According to Fig. 13a and b, none of the methods capture the behavior of the heat transfer coefficient of R1234ze(E) for vapor qualities higher than 0.4, independently of the range of heat fluxes and mass velocities. For vapor qualities lower than 0.4, it can be observed that the methods of Sun and Mishima [44], Kim and Mudawar [11] and Kanizawa et al. [1] capture the tendency of the experimental data. For the fluid R1234yf, only the method of Sun and Mishima [44] was able to adequately capture the predominance of nucleate boiling effects of the experimental data for a saturation temperature of 41 °C (see Fig. 14d). On the other hand, for a saturation temperature of 31 °C (see Fig. 13c), Saitoh et al. [15] and Kanizawa et al. [1] capture the behavior of the experimental data for vapor qualities lower than 0.4. However, none of these methods captures the predominance of convective effects and the corresponding increase of the heat transfer coefficient with increasing the vapor quality. For the isobutane (see Fig. 13e and f), the method of Kew and Cornwell [41] capture the tendency of the experimental data for a saturation temperature of 41 °C, but for a saturation temperature of 31 °C, the method underestimate the heat transfer coefficient for vapor qualities lower than 0.5.

In general, it can be concluded that the methods don't capture adequately the tendency of experimental data under conditions where convective effects are predominant. Moreover, only the method of Chen [37], Saitoh et al. [44] and Kanizawa et al. [1] consider the occurrence of surface dryout at high vapor qualities. It should be also highlighted the fact that most of the methods displayed in Fig. 13 present huge divergences from the experimental trends.

5. Heat transfer coefficient predictive method

Due to the fact that none of the predictive methods from literature was able to predict accurately the experimental data for all

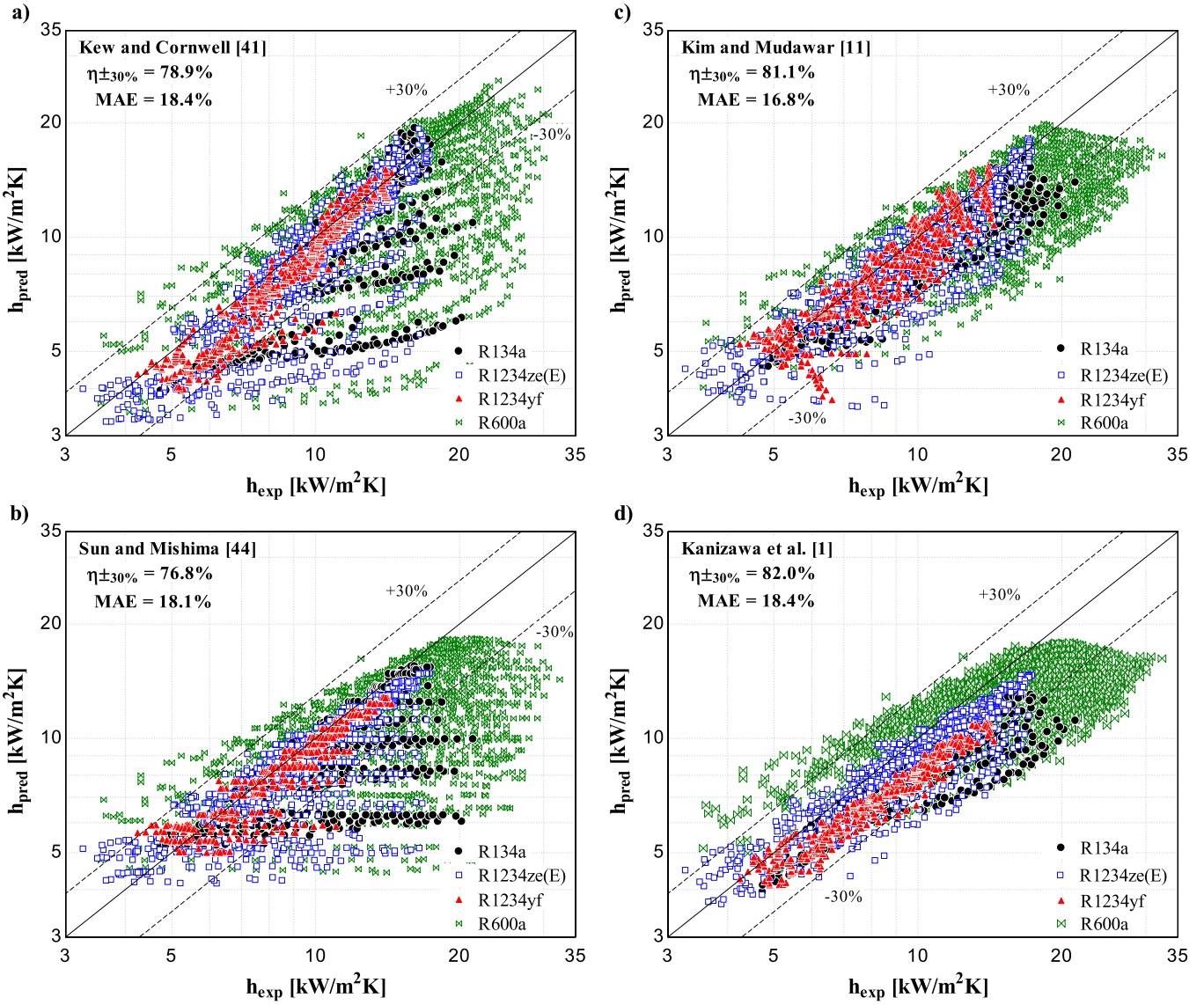

Fig. 12. Comparison of the experimental database segregated by fluids with predictive methods by: (a) Kew and Cornwell [41], (b) Sun and Mishima [44], (c) Kim and Mudawar [11] and (d) Kanizawa et al. [1].

range of conditions evaluated in the present study, in this item an updated version of the predictive method of Kanizawa et al. [1] is proposed.

5.1. Description of the updated predictive method

According to the results showed in the last section, in general, the predictive method of Kanizawa et al. [1] predicted reasonably well the experimental data for the fluids R134a, R1234ze(E) and R1234yf. However, this method failed in the prediction of the HTC under conditions where convective effects are predominant, corresponding to most of data for R600a. On the other hand, it was verified in this study that the transition between the predominance of nucleate boiling effects to convective effects occurs more abruptly than what is captured by a linear composition of these effects. Therefore, it was decided to adjust the method of Kanizawa et al. [1] by adopting an asymptotic exponent equal to two, as recommended by Liu and Winterton [39]. Therefore, the updated method for prediction of the heat transfer coefficient for vapor qualities lower than the dryout vapor quality is given as follows:

$$h_{2\phi} = \left[(F \cdot h_L)^2 + (S \cdot h_{nb})^2 \right]^{0.5} \tag{11}$$

where h_L and h_{nb} are the heat transfer coefficients related to convective and nucleate boiling effects, respectively. The HTC related to convective effects is estimated assuming only the liquid phase flowing in the tube as turbulent flow according to the correlation of Dittus and Boelter [51]. The heat transfer coefficient related to nucleate boiling effects is estimated according the correlation of Stephan and Abdelsalam [52].

The convective enhancement factor, F, and the nucleate boiling suppression factor, S, are estimated according to the correlation forms proposed for Kanizawa et al. [1], as follows:

$$F = 1 + \frac{c_{f,1} X_{tt}^{c_{f,2}}}{\left(1 + We_{uG}^{c_{f,3}}\right)} \tag{12}$$

$$S = \frac{c_{s,1} Bd^{c_{s,2}}}{1 + c_{s,3}\left(10^{-4} Re_L F^{1.25}\right)^{c_{s,4}}} \tag{13}$$

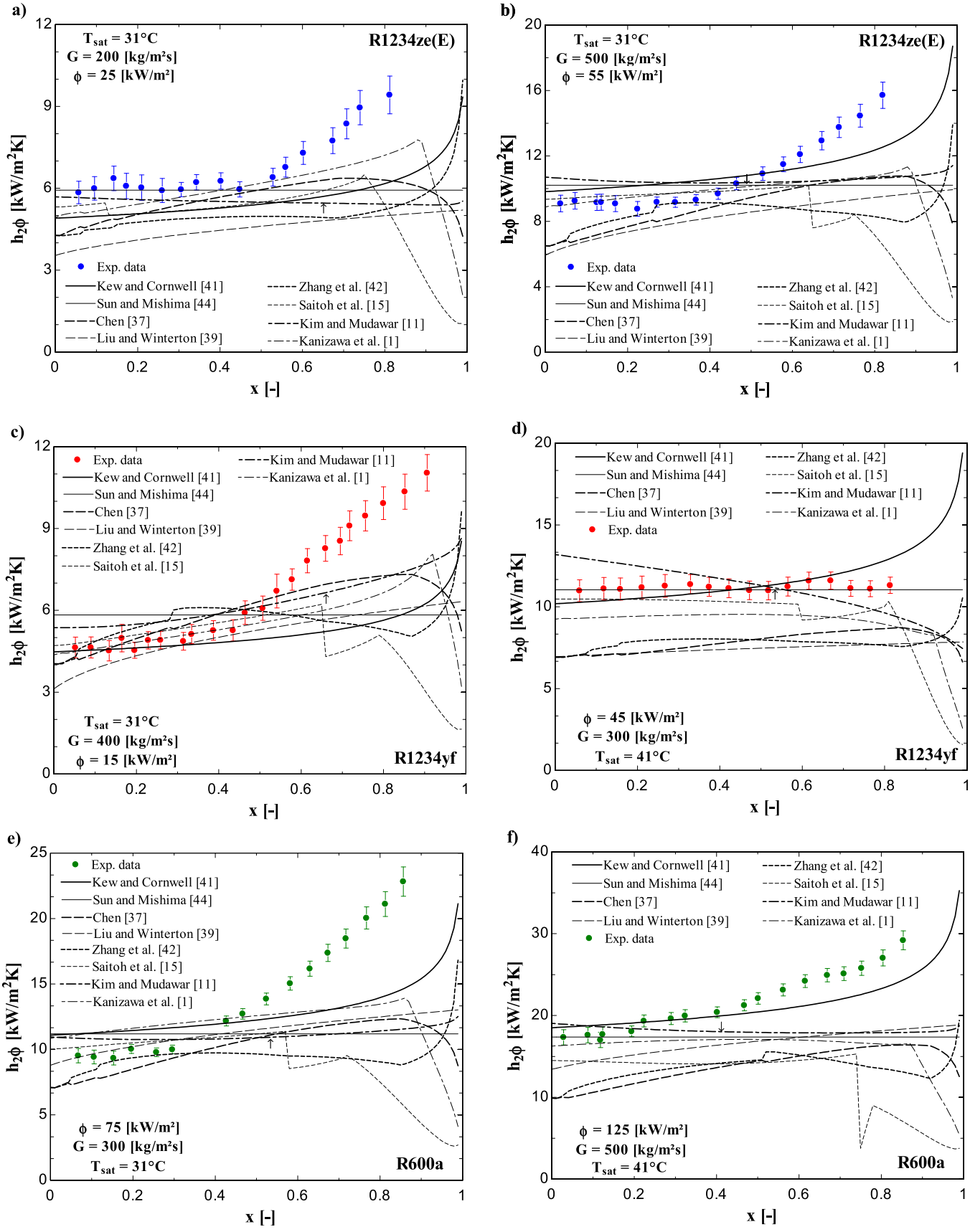

Fig. 13. Comparison of frictional pressure drop trends according to predictive methods and the experimental data for non-circular channels.

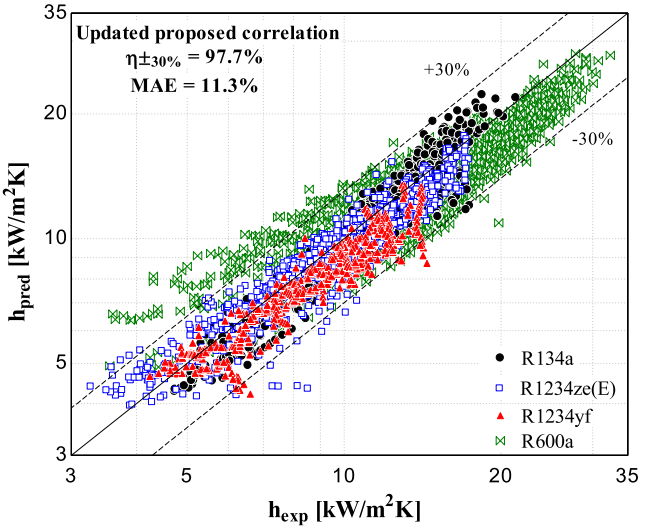

Fig. 14. Comparison of the new experimental database with the updated proposed correlation.

Table 6
Stadisticals parameters from the comparison between the present experimental data and the predictions of the developed method.[a]

Exp. database	Data points	MAE	$\eta_{30\%}$	$\eta_{20\%}$
R134a	772	**9.8%**	**100%**	**95.9%**
R1234ze(E)	847	**8.8%**	**97.8%**	**92.1%**
R1234yf	475	**10.8%**	**97.9%**	**86.1%**
R600a	1315	**14.0%**	**96.0%**	**77.0%**
Overall	3409	**11.3%**	**97.7%**	**86.3%**

[a] Bold numbers indicate a MAE below 20% and more than 80% and 70% of the data predicted within the ±30% and ±20%, respectively.

where the empirical coefficients were adjusted through the least square fitting method for non-linear equations given by the software MATLAB R2015a. Through this procedure values of $c_{f,1}$, $c_{f,2}$, $c_{f,3}$, $c_{s,1}$, $c_{s,2}$, $c_{s,3}$ and $c_{s,4}$ equal to 2.55, −1.04, −0.194, 1.427, 0.032, 0.1086 and 0.981 were found, respectively.

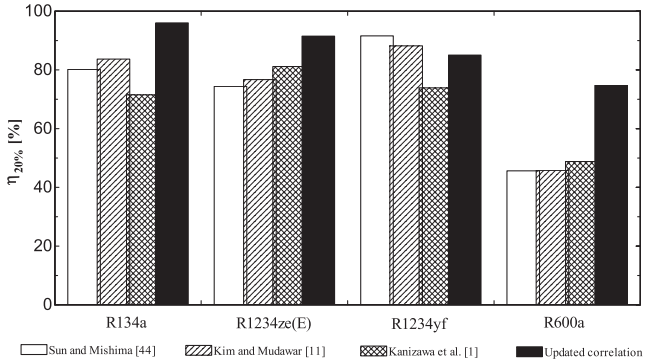

Fig. 15. Parcel of data predicted within the ±20% of error band according to predictive methods of the literature and the updated proposed method segregated by the fluid.

Considering that in the present study post-dryout experimental data were not obtained, the procedure proposed by Kanizawa et al. [1] for vapor qualities higher than the dryout ($x > x_{dryout}$) is recommended.

5.2. Evaluation of the updated predictive method

5.2.1. Statistical evaluation of the updated predictive method

Table 6 lists de mean absolute error, the parcel of data predicted within ±30% and ±20% of error band obtained from comparisons between the experimental database and the new version of the predictive method proposed originally by Kanizawa et al. [1]. According to this table, for the overall database, the method predicted almost 98% and 86% of the experimental data within error bands of ±30% and ±20%, respectively. The new method also provides accurate predictions of the particular datasets regardless of the fluid, providing values of MAE lower than 14% and $\eta_{30\%}$ higher than 95%.

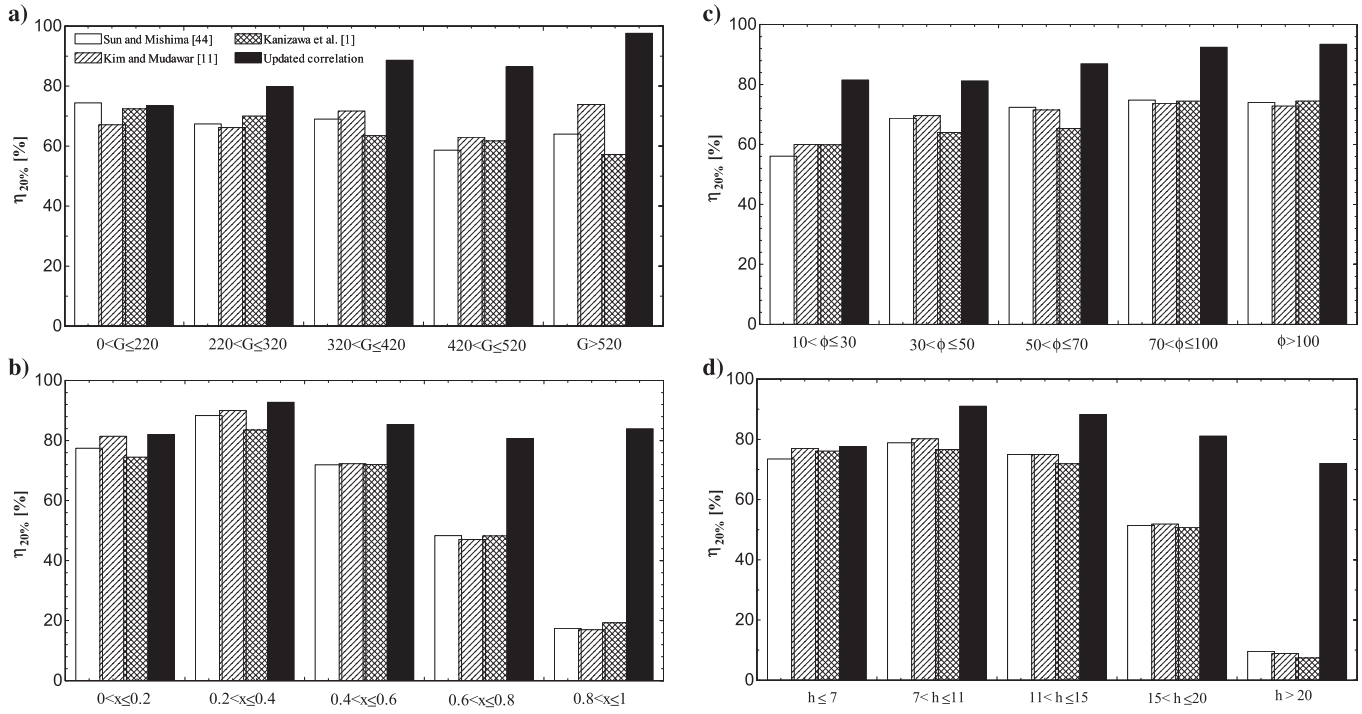

Fig. 16. Parcel of data predicted within the ±20% of error band according to (a) mass velocity, (b) vapor quality, and (c) heat flux and HTC ranges.

Table 7
Stadisticals parameters from the comparison between data from the literature and the predictions of the developed method.[a]

Author(s)	Fluid	Diameter [mm]	#Data	MAE	$\eta_{30\%}$
Tibirica and Ribatski [23]	R134a	2.32	1334	**16.0%**	**89.6%**
Anwar et al. [20]	R1234yf	1.6	200	23.1%	**89.5%**
Kanizawa et al. [1]	R134a	0.38	23	**11.9%**	**91.3%**

[a] Bold numbers indicate a MAE below 20% and more than 80% of the data predicted within the ±30%.

Fig. 14 illustrates a comparison between the experimental results and the predictions given by the modified version of the method. According to this figure, the method is reasonably accurate independently of the range of heat transfer coefficient and refrigerant.

Figs. 15 and 16 depict the parcel of experimental results predicted with an error band of ±20% according to different operational ranges for the three predictive methods from literature that provided the best predictions, according to Section 4.2, and the updated version of the method of Kanizawa et al. [1] proposed in this study.

In Fig. 15, comparisons are performed for the data segregated according to the working fluid. According to this figure, the new version provided reasonable results for the four fluids evaluated in this study, predicting more than 77% of the experimental data within an error band of ±20%. It can also be observed that the updated method improves the predictions of the original method developed by Kanizawa et al. [1]. Moreover, it is important to highlight the fact that the updated version of Kanizawa et al. [1] proposed in this study improves significantly the results for R600a, considering that the methods of literature predicted less than 50% of the experimental data within an error band of ±20%.

As shown in Fig. 16, the new version of the method predicted higher parcels of the experimental data within an error band of ±20% than the methods of Sun and Mishima [44], Kim and Mudawar [11] and Kanizawa et al. [1], regardless of the range of mass velocity,

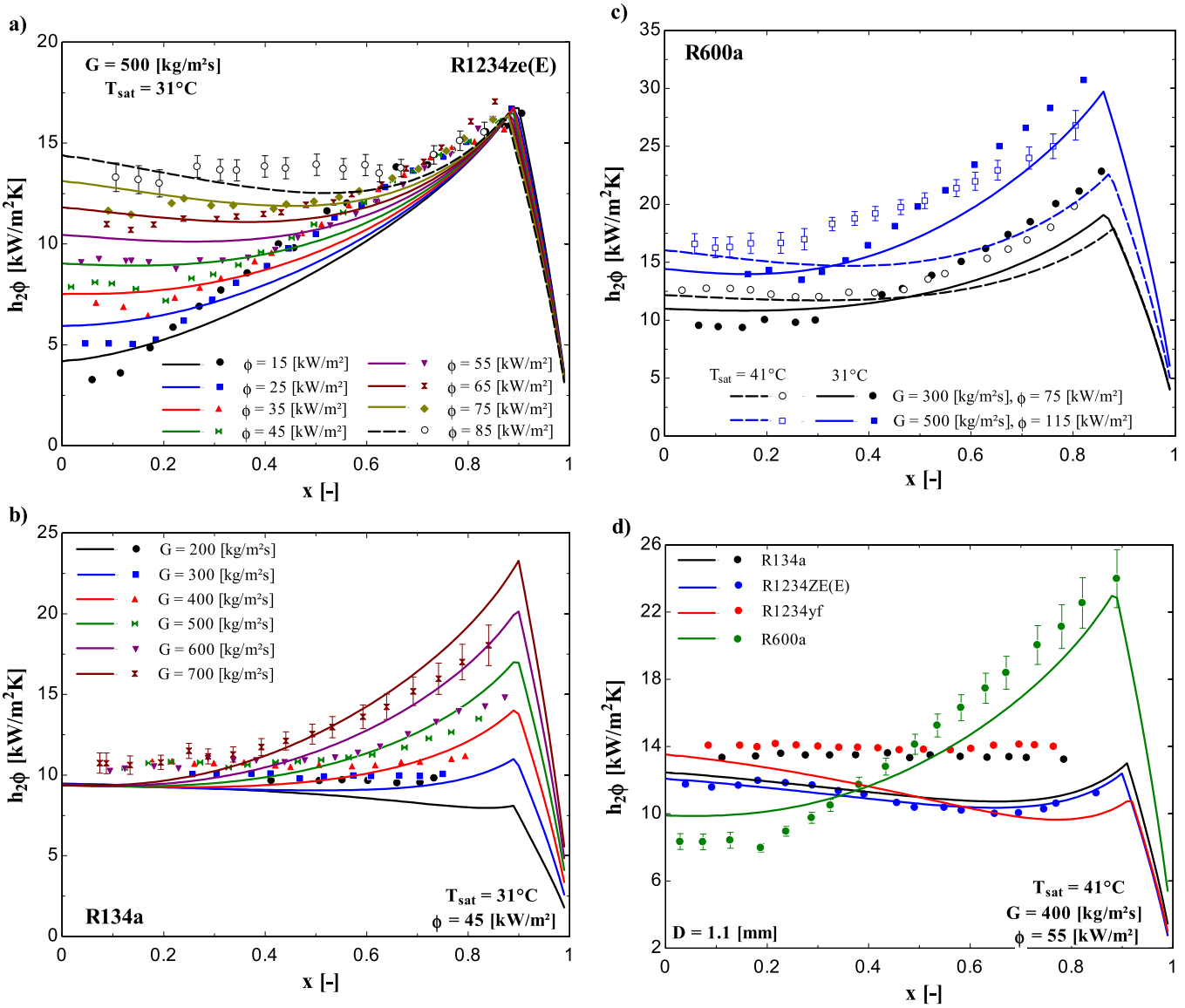

Fig. 17. Comparison between experimental data and estimated trends according to the updated version of the predictive method of Kanizawa et al. [1].

vapor quality, heat flux and heat transfer coefficient. It can also be observed that the parcel of data predicted by the updated method within an error band of ±20% does not vary significantly according to the experimental condition range, presenting values between 75 and 96%. Moreover, it is worth to mention that the updated proposed method improves considerably the predictions, compared to the methods from literature for mass velocities higher than 520 kg/m^2 s (see Fig. 16a) and for vapor qualities higher than 0.6 (see Fig. 16b). For vapor qualities higher than 0.8, the methods from literature predicted less than 25% of the experimental data within an error band of ±20%. This result can be explained by the fact that the methods from the literature do not capture satisfactorily the predominance of convective effects for vapor qualities higher than 0.4, especially for the isobutane. According to Fig. 16d, the methods of Sun and Mishima [44], Kim and Mudawar [11] and Kanizawa et al. [1], provided reasonable predictions for heat transfer coefficients lower than 15 kW/m^2 K, but failed to predict HTCs higher than 15 kW/m^2 K. On the other hand, the updated proposed method provides accurate predictions regardless the heat transfer coefficient range, improving in 800% the parcel of data predicted within an error band of ±20% for HTCs higher than 20 kW/m^2 K, corresponding to high vapor quality conditions with the refrigerant R600a.

According to Table 7, the updated version of the predictive method of Kanizawa et al. [1] predicts satisfactorily the experimental results of the independent databases of Tibirica and Ribatski [23], Anwar et al. [20] and Kanizawa et al. [1], providing more than 89% of the predictions within an error band of ±30%.

5.2.2. Parametric analysis of the updated predictive method

As shown in Fig. 17, the updated method proposed in this study is able to capture the effects of the heat flux, mass velocity, saturation temperature and working fluid on the heat transfer coefficient. Moreover, the method predicts satisfactorily the vapor quality for which the effect of the saturation temperature in the heat transfer coefficient is shifted. It can be observed that for vapor qualities lower than 0.4–0.6, according to the conditions of heat flux and mass velocity, the proposed method predicts adequately the increasing of the HTC with increasing saturation temperature. On the other hand, for high vapor qualities, the method predicts the decreasing of the heat transfer coefficient with increasing the saturation temperature. It also should be highlighted the fact that the updated proposed method predicts satisfactorily the vapor quality where the experimental HTC for isobutane overcomes the heat transfer coefficient of the fluids R134a, R1234ze(E) and R1234yf. Finally, taking into account that care was exercised during the experimental campaign in order to obtain heat transfer coefficient results for vapor qualities as closer as possible to the wall dryout, the new version of the method of Kanizawa et al. [1] seems to predict accurately the vapor quality corresponding to the onset of dryout.

6. Conclusions

The following remarks summarize the conclusions of the present investigation:

- A broad experimental database for HTC during flow boiling of R134a, R1234ze(E), R1234yf and R600a in a 1.1 mm ID tube is presented. The database comprises 3409 experimental results, heat fluxes ranging from 15 to 145 kW/m^2 K, mass velocities from 100 to 800 kg/m^2 s, saturation temperatures of 31 and 41 °C and heat transfer coefficients up to 32.4 kW/m^2.
- For experimental conditions where the nucleate boiling effects are predominant, the HTC increases with increasing the heat flux and is almost independent of the mass velocity. On the other hand, under experimental conditions where the convective effects are predominant, the HTC is independent of the heat flux and increases when increasing the mass velocity. In general, the HTC increases with increasing the saturation temperature at low vapor qualities and decreases for high vapor qualities.
- The heat transfer coefficients for R134a and R1234yf are almost similar. For low vapor qualities, the HTC of R1234ze(E) is lower than the heat transfer coefficient of R134a and R1234yf. This behavior is accentuated with increasing heat flux. For high vapor qualities, the HTC of R1234ze(E) is higher than the heat transfer coefficient of R134a. The HTC for R600a is lower than the HTC of the fluids R1234a, R1234ze(E) and R1234yf for vapor qualities lower than 0.2. However, the HTC for R600a increases drastically with increasing the vapor quality reaching values up to 120% higher than the other fluids.
- The experimental database was compared with 14 predictive methods of the literature. Statistically, the methods of Kanizawa et al. [1] and Kim and Mudawar [11] provided the best predictions of the overall database, predicting 82% and 81% of the experimental data within an error band of ±30%, respectively. In general, the predictions according to the methods of Kew and Cornwell [41] and Sun and Mishima [44] also agreed reasonably well with the experimental data for the overall database.
- In general, Kanizawa et al. [1] and Kim and Mudawar [11] provided satisfactory predictions of the data of R134a, R1234ze(E) and R1234yf. However, this methods were able to capture satisfactorily only the tendencies of the HTC with increasing the vapor quality for low and intermediate vapor qualities. None of the predictive methods was able to provide satisfactory predictions for the isobutane.
- Considering the overall analysis of the experimental data and the comparison with the predictive methods of the literature, an updated version of the predictive method of Kanizawa et al. [1] was proposed. The updated proposed version of the predictive method predicts 97.7% and 86.3% of the experimental database used on its development within an error margin of ±30% and ±20%, respectively. Moreover, the updated proposed method captures adequately the trends of the experimental data. The updated version was also able to provide satisfactory predictions of independent data from literature.

Acknowledgements

The authors gratefully acknowledge FAPESP (The State of São Paulo Research Foundation, Brazil) for the financial support under contract numbers 2010/17605-4 and 2011/50176-2 and CNPq (The National Council for Scientific and Technological Development, Brazil) for the financial support under Contract Numbers n °476763/2013-4 and 303852/2013-5. The technical support given to this investigation by Mr. José Roberto Bogni is also appreciated and deeply recognized. The authors are also grateful to Honeywell for supplying the low GWP refrigerants R1234ze(E) and R1234yf.

References

[1] F.T. Kanizawa, C.B. Tibiriçá, G. Ribatski, Heat transfer during convective flow boiling inside micro-scale channels, Int. J. Heat Mass Transf. 93 (2016) 566–583, http://dx.doi.org/10.1016/j.ijheatmasstransfer.2015.09.083.

[2] S.M. Kim, I. Mudawar, Review of databases and predictive methods for heat transfer in condensing and boiling mini/micro-channel flows, Int. J. Heat Mass Transf. 77 (2014) 627–652, http://dx.doi.org/10.1016/j.ijheatmasstransfer.2014.05.036.

[3] J.M. Calm, The next generation of refrigerants – historical review, considerations, and outlook, Int. J. Refrig. 31 (2008) 1123–1133, http://dx.doi.org/10.1016/j.ijrefrig.2008.01.013.

[4] A. Mota-Babiloni, J. Navarro-Esbrí, Á. Barragán, F. Molés, B. Peris, Drop-in energy performance evaluation of R1234yf and R1234ze(E) in a vapor compression system as R134a replacements, Appl. Therm. Eng. 71 (2014) 259–265, http://dx.doi.org/10.1016/j.applthermaleng.2014.06.056.
[5] D.F. Sempértegui-Tapia, G. Ribatski, Two-phase frictional pressure drop in horizontal micro-scale channels: experimental data analysis and prediction method development, Int. J. Multiph. Flow (2016) (in preparation).
[6] J.B. Copetti, M.H. MacAgnan, F. Zinani, Experimental study on R-600a boiling in 2.6 mm tube, Int. J. Refrig. 36 (2013) 325–334, http://dx.doi.org/10.1016/j.ijrefrig.2012.09.007.
[7] K. Choi, J. Oh, K. Saito, J. Soo, Comparison of heat transfer coefficient during evaporation of natural refrigerants and R-1234yf in horizontal small tube, Int. J. Refrig. 41 (2014) 210–218, http://dx.doi.org/10.1016/j.ijrefrig.2013.06.017.
[8] D. Del Col, M. Bortolato, S. Bortolin, Comprehensive experimental investigation of two-phase heat transfer and pressure drop with propane in a minichannel, Int. J. Refrig. 47 (2014) 66–84, http://dx.doi.org/10.1016/j.ijrefrig.2014.08.002.
[9] J.D. de Oliveira, J.B. Copetti, J.C. Passos, An experimental investigation on flow boiling heat transfer of R-600a in a horizontal small tube, Int. J. Refrig. (2016), http://dx.doi.org/10.1016/j.ijrefrig.2016.08.001.
[10] S.G. Kandlikar, P. Balasubramanian, An extension of the flow boiling correlation to transition, laminar, and deep laminar flows in minichannels and microchannels, Heat Transf. Eng. 25 (2004) 86–93, http://dx.doi.org/10.1080/01457630490280425.
[11] S.M. Kim, I. Mudawar, Universal approach to predicting saturated flow boiling heat transfer in mini/micro-channels – Part II. Two-phase heat transfer coefficient, Int. J. Heat Mass Transf. 64 (2013) 1239–1256, http://dx.doi.org/10.1016/j.ijheatmasstransfer.2013.04.014.
[12] J.R. Thome, V. Dupont, A.M. Jacobi, Heat transfer model for evaporation in microchannels. Part I: presentation of the model, Int. J. Heat Mass Transf. 47 (2004) 3375–3385, http://dx.doi.org/10.1016/j.ijheatmasstransfer.2004.01.006.
[13] K.E. Gungor, R.H.S. Winterton, Simplified general correlation for saturated flow boiling and comparisons of correlations with data, Chem. Eng. Res. Des. 65 (1987) 148–156.
[14] S. Saitoh, C. Dang, Y. Nakamura, E. Hihara, Boiling heat transfer of HFO-1234yf flowing in a smooth small-diameter horizontal tube, Int. J. Refrig. 34 (2011) 1846–1853, http://dx.doi.org/10.1016/j.ijrefrig.2011.05.018.
[15] S. Saitoh, H. Daiguji, E. Hihara, Correlation for boiling heat transfer of R-134a in horizontal tubes including effect of tube diameter, Int. J. Heat Mass Transf. 50 (2007) 5215–5225, http://dx.doi.org/10.1016/j.ijheatmasstransfer.2007.06.019.
[16] M. Li, C. Dang, E. Hihara, Flow boiling heat transfer of HFO1234yf and R32 refrigerant mixtures in a smooth horizontal tube: Part I. Experimental investigation, Int. J. Heat Mass Transf. 55 (2012) 3437–3446, http://dx.doi.org/10.1016/j.ijheatmasstransfer.2012.03.002.
[17] S. Mortada, a. Zoughaib, C. Arzano-Daurelle, D. Clodic, Boiling heat transfer and pressure drop of R-134a and R-1234yf in minichannels for low mass fluxes, Int. J. Refrig. 35 (2012) 962–973, http://dx.doi.org/10.1016/j.ijrefrig.2012.03.004.
[18] C.B. Tibiriçá, G. Ribatski, J. Richard Thome, Flow boiling characteristics for R1234ze(E) in 1.0 and 2.2 mm circular channels, J. Heat Transf. 134 (2012) 020906, http://dx.doi.org/10.1115/1.4004933.
[19] D. Del Col, S. Bortolin, D. Torresin, A. Cavallini, Flow boiling of R1234yf in a 1 mm diameter channel, Int. J. Refrig. 36 (2013) 353–362, http://dx.doi.org/10.1016/j.ijrefrig.2012.10.026.
[20] Z. Anwar, B. Palm, R. Khodabandeh, Flow boiling heat transfer, pressure drop and dryout characteristics of R1234yf: experimental results and predictions, Exp. Therm. Fluid Sci. 66 (2015) 137–149, http://dx.doi.org/10.1016/j.expthermflusci.2015.03.021.
[21] M.M. Mahmoud, T.G. Karayiannis, Heat transfer correlation for flow boiling in small to micro tubes, Int. J. Heat Mass Transf. 66 (2013) 553–574, http://dx.doi.org/10.1016/j.ijheatmasstransfer.2013.07.042.
[22] H. Huang, N. Borhani, J.R. Thome, Experimental investigation on flow boiling pressure drop and heat transfer of R1233zd(E) in a multi-microchannel evaporator, Int. J. Heat Mass Transf. 98 (2016) 596–610, http://dx.doi.org/10.1016/j.ijheatmasstransfer.2016.03.051.
[23] C.B. Tibiriçá, G. Ribatski, Flow boiling heat transfer of R134a and R245fa in a 2.3mm tube, Int. J. Heat Mass Transf. 53 (2010) 2459–2468, http://dx.doi.org/10.1016/j.ijheatmasstransfer.2010.01.038.
[24] D. Sempértegui-Tapia, J. De Oliveira Alves, G. Ribatski, Two-phase flow characteristics during convective boiling of halocarbon refrigerants inside horizontal small-diameter tubes, Heat Transf. Eng. 34 (2013) 1073–1087, http://dx.doi.org/10.1080/01457632.2013.763543.
[25] F.T. Kanizawa, G. Ribatski, A new void fraction predictive method based on the minimum energy dissipation, J. Braz. Soc. Mech. Sci. Eng. (2015), http://dx.doi.org/10.1007/s40430-015-0446-x.
[26] S.M. Zivi, Estimation of steady-state steam void-fraction by means of the principle of minimum entropy production, J. Heat Transf. 86 (1964).
[27] H. Müller-Steinhagen, K. Heck, A simple friction pressure drop correlation for two-phase flow in pipes, Chem. Eng. Process. Process Intensif. 20 (1986) 297–308, http://dx.doi.org/10.1016/0255-2701(86)80008-3.
[28] H. Blasius, Das ahnlichkeitsgesetz bei reibungsvorg/ingen in fltissigkeiten, Forschg. Arb. Ing. Wes. 131 (1913).
[29] R. Siegel, E.M. Sparrow, T.M. Hallman, Steady laminar heat transfer in a circular tube with prescribed wall heat flux, Appl. Sci. Res. Sect. A 7 (1958) 386–392, http://dx.doi.org/10.1007/BF03184999.
[30] V. Gnielinski, New equations for heat and mass transfer in turbulent flow in pipes and channels, Int. Chem. Eng. 359–368 (1976).
[31] R.B. Abernethy, B.D. Powell, D.L. Colbert, D.G. Sanders, J.W. Thompson Jr., Handbook Uncertainty in Gas Turbine Measurements, Arnold Eng, Tennessee, 1973.
[32] B.N. Taylor, C.E. Kuyatt, Guidelines for Evaluating and Expressing the Uncertainty of NIST Measurement Results, NIST Tech. Note. (1994) 25.
[33] C.B. Tibiriçá, G. Ribatski, Flow patterns and bubble departure fundamental characteristics during flow boiling in microscale channels, Exp. Therm. Fluid Sci. 59 (2014) 152–165, http://dx.doi.org/10.1016/j.expthermflusci.2014.02.017.
[34] A. Kalani, S.G. Kandlikar, Flow patterns and heat transfer mechanisms during flow boiling over open microchannels in tapered manifold (OMM), Int. J. Heat Mass Transf. 89 (2015) 494–504, http://dx.doi.org/10.1016/j.ijheatmasstransfer.2015.05.070.
[35] S. Basu, B. Werneke, Y. Peles, M.K. Jensen, Transient microscale flow boiling heat transfer characteristics of HFE-7000, Int. J. Heat Mass Transf. 90 (2015) 396–405, http://dx.doi.org/10.1016/j.ijheatmasstransfer.2015.06.038.
[36] C.A. Chávez, H.L.S.L. Leão, G. Ribatski, Evaluation of thermal-hydraulic performance of hydrocarbon refrigerants during flow boiling in a microchannels array heat sink, Appl. Therm. Eng. 111 (2017) 703–717, http://dx.doi.org/10.1016/j.applthermaleng.2016.09.109.
[37] J.C. Chen, Correlation for boiling heat transfer to saturated fluids in convective flow, Ind. Eng. Chem. Process Des. Dev. 5 (1966) 322–329, http://dx.doi.org/10.1021/i260019a023.
[38] G.M. Lazarek, S.H. Black, Evaporative heat transfer, pressure drop and critical heat flux in a small vertical tube with R-113, Int. J. Heat Mass Transf. 25 (1982) 945–960, http://dx.doi.org/10.1016/0017-9310(82)90070-9.
[39] Z. Liu, R.H.S. Winterton, A general correlation for saturated and subcooled flow boiling in tubes and annuli, based on a nucleate pool boiling equation, Int. J. Heat Mass Transf. 34 (1991) 2759–2766, http://dx.doi.org/10.1016/0017-9310(91)90234-6.
[40] T.N. Tran, M.W. Wambsganss, D.M. France, Small circular- and rectangular-channel boiling with two refrigerants, Int. J. Multiph. Flow 22 (1996) 485–498.
[41] P.A. Kew, K. Cornwell, Correlations for the prediction of boiling heat transfer in small-diameter channels, Appl. Therm. Eng. 17 (1997) 705–715, http://dx.doi.org/10.1016/S1359-4311(96)00071-3.
[42] W. Zhang, T. Hibiki, K. Mishima, Correlation for flow boiling heat transfer in mini-channels, Int. J. Heat Mass Transf. 47 (2004) 5749–5763, http://dx.doi.org/10.1016/j.ijheatmasstransfer.2004.07.034.
[43] S.S. Bertsch, E.A. Groll, S.V. Garimella, A composite heat transfer correlation for saturated flow boiling in small channels, Int. J. Heat Mass Transf. 52 (2009) 2110–2118, http://dx.doi.org/10.1016/j.ijheatmasstransfer.2008.10.022.
[44] L. Sun, K. Mishima, An evaluation of prediction methods for saturated flow boiling heat transfer in mini-channels, Int. J. Heat Mass Transf. 52 (2009) 5323–5329, http://dx.doi.org/10.1016/j.ijheatmasstransfer.2009.06.041.
[45] W. Li, Z. Wu, A general correlation for evaporative heat transfer in micro/mini-channels, Int. J. Heat Mass Transf. 53 (2010) 1778–1787, http://dx.doi.org/10.1016/j.ijheatmasstransfer.2010.01.012.
[46] G.R. Warrier, V.K. Dhir, L.A. Momoda, Heat transfer and pressure drop in narrow rectangular channels, Exp. Therm. Fluid Sci. 26 (2002) 53–64, http://dx.doi.org/10.1016/S0894-1777(02)00107-3.
[47] H.K. Oh, C.H. Son, Evaporation flow pattern and heat transfer of R-22 and R-134a in small diameter tubes, Heat Mass Transf. Und Stoffuebertragung. 47 (2011) 703–717, http://dx.doi.org/10.1007/s00231-011-0761-4.
[48] J.T. Oh, A.S. Pamitran, K.I. Choi, P. Hrnjak, Experimental investigation on two-phase flow boiling heat transfer of five refrigerants in horizontal small tubes of 0.5, 1.5 and 3.0 mm inner diameters, Int. J. Heat Mass Transf. 54 (2011) 2080–2088, http://dx.doi.org/10.1016/j.ijheatmasstransfer.2010.12.021.
[49] A. Cioncolini, J.R. Thome, Algebraic turbulence modeling in adiabatic and evaporating annular two-phase flow, Int. J. Heat Fluid Flow 32 (2011) 805–817, http://dx.doi.org/10.1016/j.ijheatfluidflow.2011.05.006.
[50] E. Costa-Patry, J.R. Thome, Flow pattern-based flow boiling heat transfer model for microchannels, Int. J. Refrig. 36 (2013) 414–420, http://dx.doi.org/10.1016/j.ijrefrig.2012.12.006.
[51] F.W. Dittus, L.M.K. Boelter, Heat transfer in automobile radiators of the tubular type, Int. Commun. Heat Mass Transf. 12 (1985) 3–22, http://dx.doi.org/10.1016/0735-1933(85)90003-X.
[52] K. Stephan, M. Abdelsalam, Heat-transfer correlations for natural convection boiling, Int. J. Heat Mass Transf. 23 (1980) 73–87, http://dx.doi.org/10.1016/0017-9310(80)90140-4.